Alexandria Engineering Journal (2022) 61, 3959–3969

HOSTED BY

Alexandria University

Alexandria Engineering Journal

www.elsevier.com/locate/aej
www.sciencedirect.com

Grasping posture of humanoid manipulator based on target shape analysis and force closure

Ying Liu [a], Du Jiang [a,b,c,*], Bo Tao [a,b,c,*], Jinxian Qi [a], Guozhang Jiang [c], Juntong Yun [a], Li Huang [e,f], Xiliang Tong [a,b], Baojia Chen [d], Gongfa Li [a,b,c,*]

[a] *Key Laboratory of Metallurgical Equipment and Control Technology of Ministry of Education, Wuhan University of Science and Technology, Wuhan 430081, China*
[b] *Research Center for Biomimetic Robot and Intelligent Measurement and Control, Wuhan University of Science and Technology, Wuhan 430081, China*
[c] *Hubei Key Laboratory of Mechanical Transmission and Manufacturing Engineering, Wuhan University of Science and Technology, Wuhan 430081, China*
[d] *Hubei Key Laboratory of Hydroelectric Machinery Design& Maintenance, Three Gorges University, Yichang 443002, China*
[e] *College of Computer Science and Technology, Wuhan University of Science and Technology, Wuhan 430081, China*
[f] *Hubei Province Key Laboratory of Intelligent Information Processing and Real-time Industrial System, Wuhan University of Science and Technology, Wuhan 430081, China*

Received 12 August 2021; revised 1 September 2021; accepted 9 September 2021
Available online 21 September 2021

KEYWORDS

Force closed;
Humanoid manipulator;
Grasping posture;
Target form analysis;
CPC algorithm

Abstract With the diversity of manipulator grasping methods and the complexity of the unstructured environment, the grasping planning of the target object is very complicated. However, the external factor for the manipulator grasping is primarily the external shape of the target object. Therefore, it is of great significance to establish a grasping system based on target shape analysis. This paper proposes a method for determining the grasping posture of manipulator based on shape analysis and force closure. The irregular or complex objects are reduced to a combination of some basic shapes. The 3D data points of the object are split into blocks and each part is fitted to sphere, cylinder or rectangle by a best-fit algorithm. This allows the grasping posture of the manipulator to be determined quickly. The grasping characteristics of the object are analyzed and the grasping surface is described qualitatively by means of a superellipse. The grasping of objects is simplified according to the stable grasping condition of force closure. The force spiral space for grasping defines the grasping quality of the manipulator. The best grasping posture is obtained by evaluating the indicators. This method eliminates complex training processes, reduces the complexity of robotic grasping and highly universal.

* Corresponding authors at: Key Laboratory of Metallurgical Equipment and Control Technology of Ministry of Education, Wuhan University of Science and Technology, Wuhan 430081, China.
E-mail addresses: jiangdu@wust.edu.cn (D. Jiang), taoboq@wust.edu.cn (B. Tao), ligongfa@wust.edu.cn (G. Li).

Peer review under responsibility of Faculty of Engineering, Alexandria University.

https://doi.org/10.1016/j.aej.2021.09.017

1. Introduction

The developmental degree of industrial robots has matured and they are mainly used to manufacturing in the factory floor. However, they cannot achieve independent recognition, planning, and motion [1,2]. The other developmental direction of robots, intelligent robots, is relatively in a flourishing stage, which is also a research direction of interest for scholars and research institutes [3,4]. Intelligent robots are used in a wide range of applications, such as space maintenance, services, healthcare, agriculture and animal husbandry [5-7]. Compared to industrial robots, intelligent robots are used in complex and uncertain environments, which require intelligent robots to have autonomous identification, planning and operation. Since the 1960s, robots have developed rapidly. However, in recent years, more and more scholars and experts have started to research in the field of intelligent robots [8,9].

Manipulators are the core component of intelligent robots that are as flexible and delicate as human hands [10]. It has a very fine mechanical structure, which makes them much maneuverability. But on the other hand, it also makes the control of the manipulator more complex [11]. It is able to grasp and manipulate objects flexibly to achieve its autonomous dexterity [12,13]. The grasping planning of a manipulator includes the analysis of itself and the analysis of the target object. They include the body analysis of the object, mathematical model building, contact position planning, gripping posture and grasping force planning [14].

Grasping planning based on model analysis methods is not only relevant for object attribute recognition, but also for shape analysis of the target object. This has always been a big challenge, so the shape analysis of the target object is crucial important. Using the concave and convex properties of the object, the constrained planar cuts (CPC) method is used to segment the target object in this paper and fit it to a basic shape. The complexity of the grasping analysis is reduced and the grasping pose of the object is determined quickly. A method for determining the gripping pose of a manipulator based on shape analysis and force closure is presented in this paper. Based on the basic shape, the characteristic planes of the object are analyzed. A mechanical model of the grasping contact points is built to obtain the optimal grasping pose. The complex training process of this method is eliminated and the grasping complexity of the manipulator is reduced.

The reminder of the paper is as follows. The main approaches to robotic grasp planning are reviewed in second section, including data-driven approaches and model analysis methods. The third section segmentation and fitting of the target shape is described and a CPC algorithm for concave and super clustering to simplify complex objects is presented. In fourth section, we determine the grasping pose based on shape analysis and force closure. In section fifth, we give the results and analysis of the grasp planning experiments. See section sixth for conclusions.

2. Related works

The whole process of gripping the initial state to reaching the target state after grasping the object is covered by grasping planning, which involves many aspects, such as sensors and posture planning [15,45]. The complex structure of the manipulator is made more difficult to adapt by the traditional simple control model. By building complex grasping models, it involves object mathematical model construction, fingertip contact position planning, palm grasping posture and joint grasping force planning [16]. According to the current state of research, there are two main types of grasping planning for manipulators, namely data-driven method and model analysis method [17].

The data-driven approach is based on perceptual information and a priori knowledge to achieve dexterous hand grasp planning with the help of machine learning [18,46]. In recent years, the approach has been gradually applied to intelligent robot grasp planning tasks with certain results [19,42]. It focuses on solving the problem of target object model and environment perception understanding. Human-captured perceptual data and a priori knowledge complete the mastery autonomous planning [20].

Visual information extraction of the target external representations has been attempted by many researchers, with attributes such as shape, size, color etc. A new image feature was devised by Lenz et al. [21], which was extracted from training data. A grasping probability model was trained to accomplish the task of learning target object grasping points from images, which was eventually successfully implemented in real scenarios. A new shape-based descriptor was proposed by Bohg et al [19]. Global features of the target object in the image can be expressed to enable the training of a grasp point classifier model. The multi-touch grasp of a robot learns to calculate the position of each finger contact point with the target [22].

The core of the model analysis approach is analyzed the properties of the manipulator and the target object [23,24], and to create a physical model, as shown in Fig. 1. Kinematic, dynamical model and contact physical models of the manipulator create its grasping [25]. Based on the grasping task, the parameters are evaluated as optimization targets for the grasping model and an objective optimization function is created. The best grasping model is selected using a global optimization approach to achieve a grasping operation planning manipulator [28].

Looking back at the history of analysis, Mason and Salisbury's concepts of 'force closure' and 'formal closure' were first introduced [29]. The preconditions for force closure and formal closure grasping were verified by them. It became the theoretical basis for planning-based grasping. On the basis of this, Kerr and Roth further developed the concepts of "gripping force" and "manipulation force" [30].

A method to optimize the position and force in force closure grippers was presented [31]. The combined problem of force closure gripping is simplified to a bilinear matrix inequality (BMI). An efficient solution method based on semi-definite programming was proposed. By maximizing a lower bound on the grasping degree, the quality of the grasp can be improved. A geometric framework to solve two common pose estimation problems was proposed [32]: a geometric problem using two reference direction measurements, and a geometric kinematic problem using a single reference direction measurement and velocity measurement. Both problems can be expressed as angular optimization problems, and an exact closed-form solution can be obtained by solving the angular optimization problem. Transformed the grasping problem into an optimization problem, and proposed an improved comprehensive method of high-quality grasping based on genetic algorithm [33]. By

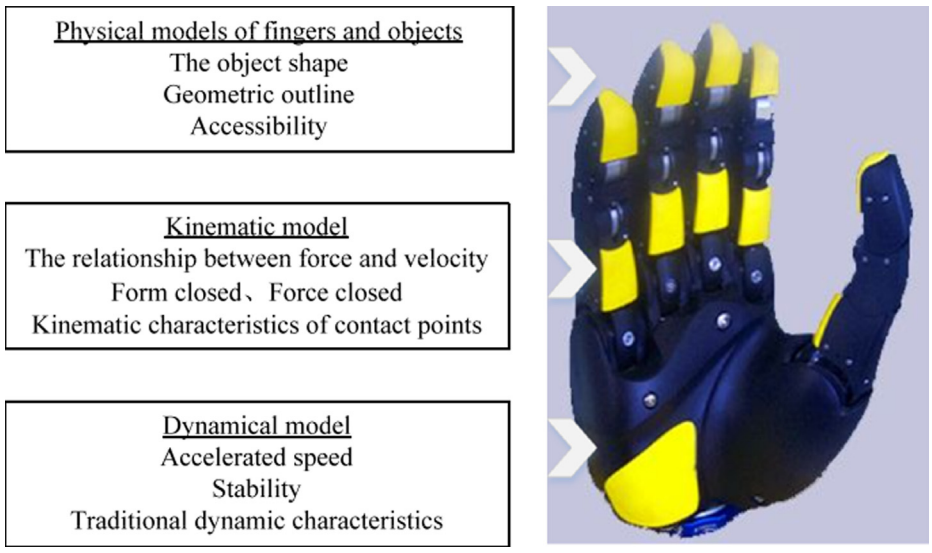

Fig. 1 Problems of analysis and operation.

generating force spiral populations, the quality of initial feasible grasping is improved.

The kinematics and grasping problems of the SCARA vacuum manipulator are studied [34], and the joint coordinate system of the manipulator is established by the MDH method. The string position method is used to complete the inverse kinematics solution, thereby realizing the grasping task of the manipulator. A general dynamic force distribution (DFD) algorithm suitable for multi-finger grasping is proposed [35]. The determination of the contact force is divided into two stages: the direction of the optimal internal force is determined in the grasping planning, and the control force and compensation factor are determined during task manipulation. The algorithm can deal directly with non-linear and coupling constraints, and overcomes temporal discontinuities very well. Nonlinear programming is the object of study [36], and a solver with fmincon as the core function is built to solve nonlinear programming problems. This algorithm can realize autonomous grasping. The grasping force calculation problem of anthropomorphic hands is studied [37], and an algorithm solution suitable for online implementation is proposed, which dynamically reduces the number of active torque constraints and greatly reduces the calculation load. A grasping algorithm based on multiple geometric constraints is proposed [38], which is mainly aimed at the problem that the robot is difficult to grasp autonomously in a random environment. This algorithm can be applied to a wide variety of target captures that lack the original model, and it has a certain generalization.

The data-driven approach requires a robot with fine-grained perception capabilities and a large amount of training data, with low adaptability. However, the approach of model analysis does not require the creation of a special database and its methods are highly versatile. This crawl planning takes into account the entire crawl process and it can be used for practically different crawl tasks.

3. Method

The idea of segmenting and then fitting is adopted in this article, and complex objects with irregular shapes are transformed into a combination of basic shapes. The specific method is that the concavity and super-body clustering CPC algorithm is adopted, and then the three-dimensional point cloud of the captured object is divided into smaller parts. According to the best fitting algorithm of the evaluation function, a sphere, cylinder or cuboid is fitted by the point cloud. In this way, complex and irregular objects can be simplified into a combination of several basic shapes, and subsequent grasping planning becomes convenient. The specific algorithm steps are shown in Fig. 2.

3.1. Target model segmentation based on CPC

The segmentation algorithm is specifically the CPC algorithm in this paper [44]. The segmentation object of this method is grab the object, the object itself is segmented when the robot

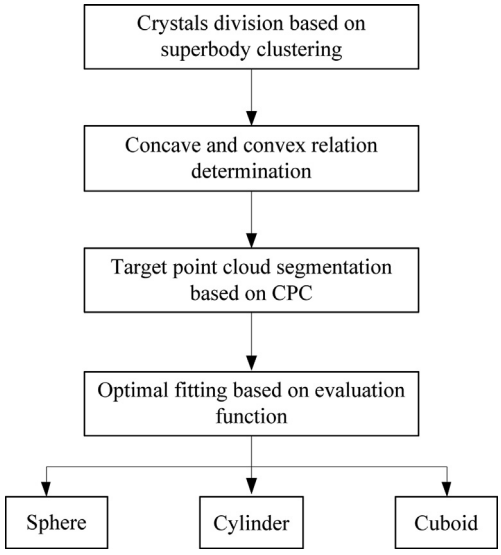

Fig. 2 Block diagram of segmentation and simplification algorithm of target point cloud.

grabs the object. In order to obtain different regions, the CPC algorithm is used to segment the target point cloud [39], and the target object is divided into different regions for the analysis of the target object shape. The following is the specific method:

1) Over-segmentation of superbody clustering. Supervoxel is collection of "body", whose elements are squares essentially. The purpose of superbody clustering is over-segment the point cloud, Many small blocks with no actual physical meaning are turned into the target object point cloud,instead of segmenting specific objects [26].

2) Judgment of concave-convex relation. The concave-convex relationship is judged by the extended convexity criterion (CC). The core of CC is used the angle α formed by the line between the centers of two adjacent areas and the normal vector of each area to judge. Fig. 3 shows the schematic diagram based on the concave-convexity relation determination of CC. If $\alpha_1 > \alpha_2$, the two regions is concave. If $\alpha_1 < \alpha_2$, the two regions is convex. Comparing α directly is more complicated, and the normal vector and the volumetric centroid vector can be introduced. If Eq. (1) is true, it is convex. If Eq. (2) is true, then it is concave.

$$n_1 \cdot d - n_2 \cdot d \geqslant 0 \tag{1}$$

$$n_1 \cdot d - n_2 \cdot d < 0 \tag{2}$$

In which, $d = \frac{x_1 - x_2}{\|x_1 - x_2\|_2}$, x is the body diathesis heart vector, n is the normal vector of voxel surface.

3) The target point cloud segmentation of CPC. After obtaining the concavity and convexity, the target point cloud is segmented by CPC semi-global segmentation. The specific operation steps are as follows:

(a) Obtain the Euclidean edge cloud (EEC). At the edges connecting the supervoxels, the object is cut. Therefore, the adjacency graph is first transformed into EEC, which each point represents an edge in the adjacent graph. The average value (x_1, x_2) of their connected supervoxels is set by the point coordinates. In addition, they are consistent with the angle (n_1, n_2) between the normal of the two super voxels.

(b) Geometrically constrained partitioning. The cut parts are searched by the partition model of EEC geometric constraints. In order to find the cutting plane, the local constraint, direction-weighted random sample consensus (RANSAC) algorithm is introduced and applied to the edge cloud.

(c) Locally constrained cutting. Although multiple parts of the concave surface can be separated by this algorithm, but sometimes it is cut that the strongly concave area causes the whole. To prevent this over-segmentation, the cutting is limited to the area near the local concave surface. Edge points

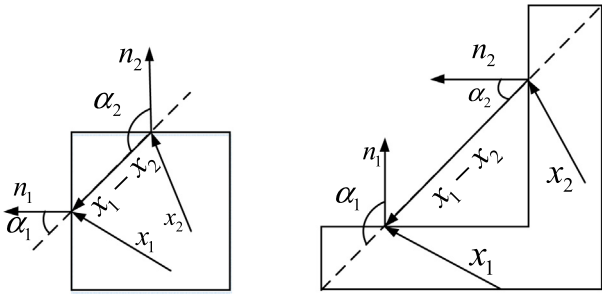

Fig. 3 Convex determination principle.

P_m within a set of model regions were obtained and they were Euclidian Clustered over a clustering threshold equal to the super voxel seed size $P_m^n \subset P_m$ denotes the set of points in the nth cluster such that it cuts on the local cluster rather than on P_m.

(d) The purpose of cutting is to simplify the target model, not to segment it in the precise sense. Therefore, block cuts should be avoided in terms of parameter settings. In this paper, the algorithm successfully divides each main part of the object, and the segmentation results are shown in Fig. 4.

3.2. Optimal fitting of basic shape

By constructing a basic shape target model, we can grasp and plan complex objects. The accuracy of the shape fitting is compared to the accuracy of the matching when the model is simplified. The former has a greater impact on the development of robotic grasping strategies. This section describes each point cloud block from the previous section. The point cloud blocks are fitted to spheres, cylinders or rectangles using an evaluation algorithm with an evaluation function. The evaluation function for each fitted shape is focused on to determine the best fit.

1) Sphere fitting. The parameters of sphere fitting are center $c(c_x, c_y, c_z)$ and radius r. Let Q be the point set of some points(x_i, y_i, z_i). q_i is any point among them, and n is the number of points in the point set. The expression equation of a general sphere is as follows:

$$(x_i - c_x)^2 + (y_i - c_y)^2 + (z_i - c_z)^2 - r^2 = 0 \tag{3}$$

The degree of sphere fitting is determined by calculating the Euclidean Distance from each point in Q to the surface of the fitted sphere. The existing algorithm of PCL point cloud database was used to achieve the sphere fitting, and the optimal center $c(c_x, c_y, c_z)$ and radius r of the sphere were obtained.

The evaluation function is the sum of the errors from all points in each segment to the center of the fitted circle. The specific formula is as follows:

$$L_q = \sum_{i=1}^{n} (\| q_i - c \|_2 - r) \tag{4}$$

2) Cylindrical fitting. At present, the least square method is used to realize the cylinder fitting. The core idea is to minimize the sum of the distance from the discrete point to the central axis of the cylinder and the radius of the fitted cylinder.

Similarly, PCL point cloud database with existing algorithms to fit optimal columns, and obtain the coordinates of the central axis midpoint v_0, the length d_z and the radius r of the cylinder. The difference sum of Euclidean Distances between all points in Q and the cylinder surface is also used as the evaluation function. The formula is shown in Eq. (6). It is worth noting that it needs to be determined whether the point is on the cylinder or on the end face. θ represents the angle of connection between point q_i and v_0 on point cloud Q and the central axis n_a, θ_d represents the angle of v_0 and the line between the boundary of two underlying circles and the central axis n_a. If $\theta > \theta_d$, the point is on the cylinder, otherwise the point is on the end face. The formula is shown in Eq. (5).

$$\sigma_i = \begin{cases} \|q_i - v_0\|_2 \cdot \sin\theta - r, & if\theta > \theta_d \\ \|q_i - v_0\|_2 \cdot \cos\theta - \frac{d_z}{2}, & if\theta \leq \theta_d \end{cases} \tag{5}$$

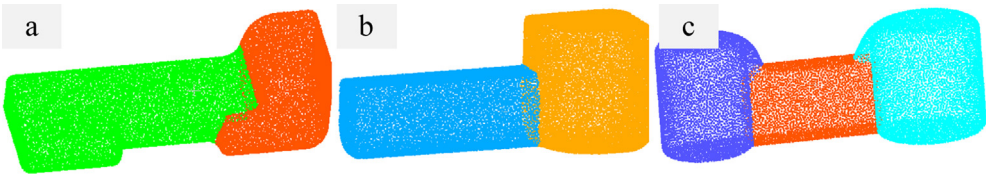

Fig. 4 Target object segmentation results based on CPC method (a: Object 1, b: Object 2, c: Object 3).

$$L_z = \sum_{i=1}^{n} |\sigma_i| \tag{6}$$

In which, L_z is the evaluation function of cylinder.

3) Cuboid fitting. The fitting process of cuboid is complicated, so bounding box is introduced here to simplify it. The rectangular parallelepiped is fitted by performing oriented bounding box (OBB) processing on the point cloud [43]. The OBB processing will make the final fitting result completely surround the original point cloud.

The fitting cuboid is evaluated by the Eq. (7) evaluation function L_c.

$$L_c = \sum_{i=1}^{n} \sum_{k=1}^{3} \min |d_{0k} \cdot \sin\theta_k|, \text{ if } u_{0k} \in l_k \tag{7}$$

In which, k is the number of three non-parallel faces in a cuboid. u_{0k} is the intersection point of C_0, and the center point of a cuboid k.

The distance between u_{0k} and the four edges and corners of l_k is used to judge whether u_{0k} is in the plane l_k. d_{0k} denotes the distance between the intersection point of the center point of the cuboid C_0 and any point q_i in the point cloud Q and the two parallel surfaces l_k and l_{k2}. θ_k is the angle of C_0 and q_i on the same plane of the line central point l_k and any point l_{k2} of the point cloud.

With the method described above, evaluation functions based on the sum of distance differences for spheres, cylinders and rectangles are obtained. Then, three basic shapes were successively fitted for each point cloud area. Based on the evaluation function, the fit with the lowest value L of the fit evaluation function was selected as the best fit. Finally, the form analysis of the three target objects is carried out, and the final result is shown in Fig. 5.

4. Determination of grasping posture based on shape analysis and force closure

4.1. Analysis of object feature plane and grasping plane

When the hand makes a grasping action, it can adjust the grip of the palm to the shape of the object. Therefore it is important to first determine the grasping pattern of the hand, which can positively contribute to the grasping of a humanoid robot hand [41]. The gripping experience of the human hand and the maximum gripping space of the robot are considered, as shown in Fig. 6(a). The initial gripping position of the robot is best when the YZ plane of the thumb joint of the robot is parallel to the table. As shown in Fig. 6(b), the X-direction is the direction of the manipulator when it enters the grasping.

The characteristic surface of the basic body can be established from the optimal grasping plane of the humanoid manipulator [27]. The feature plane is used for grasping the plane of the manipulator finger, which is also the plane formed by the contact point between the five fingers and the object. It can be seen that the feature plane is perpendicular to the captured basic shape, so the general basic body has its own feature plane, as shown in Fig. 7. The yellow solids represent the basic bodies and the green planes represent the feature planes.

The characteristic plane of a sphere is generally any cross-section through the center of the sphere. The characteristic plane of a rectangular body is a plane passing through the center of mass and perpendicular to three sets of complementary parallel planes. The characteristic plane of a cylinder is any cross-section perpendicular to the cylindrical axis. In general, the characteristic plane through the center of mass is the most appropriate.

The optimal grasping plane of the manipulator and the characteristic plane of the basic shape can be combined to form the grasping plane of the object. We can reduce grasping points in three dimensions to learning in two dimensions, and three or more grasping points can be reduced to a flat geometric space.

The contour line formed by the intersection of the feature plane and the outer contour of the object can be expressed by the superellipse function. The position of the contact point on the surface of the object can also be expressed by the superellipse. In general, the parameters of the superellipse can be expressed as Eq. (8).

$$\begin{cases} x(\omega) = a_x \cos^{\varepsilon}\omega \\ y(\omega) = b_y \sin^{\varepsilon}\omega \end{cases}, -\pi \le \omega \le \pi \tag{8}$$

In which, a_x and b_y represent the semi-axis length of the superellipse, ε controls the shape of the curve on the characteristic surface.

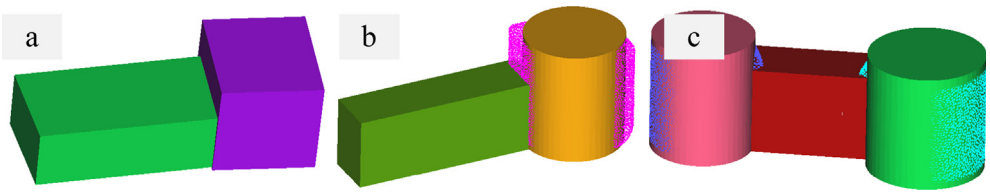

Fig. 5 Final result of basic shape fitting (a: Object 1, b: Object 2, c: Object 3).

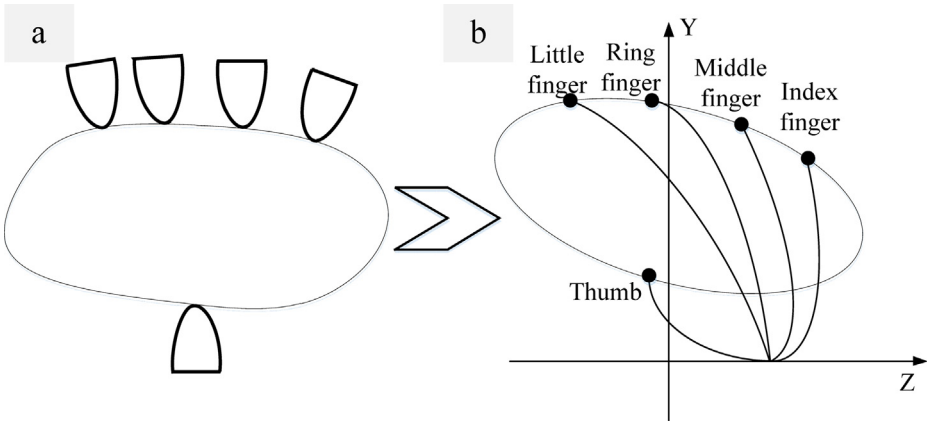

Fig. 6 Optimal grasping plane of humanoid manipulators.

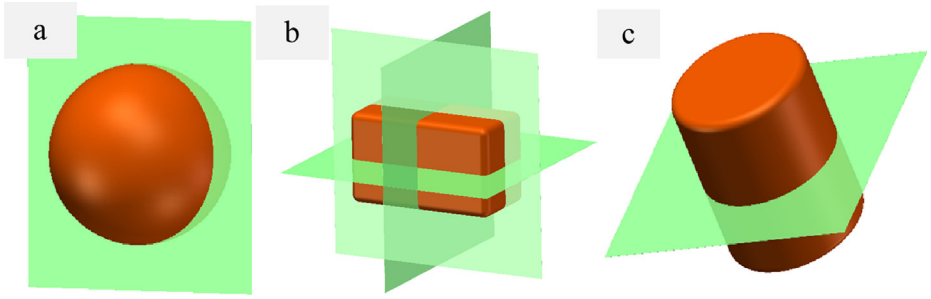

Fig. 7 Characteristic plane of the three basic bodies (a: Spherical, b: Rectangular, c: Cylinder).

According to the characteristics of the superellipse, it can be known that most convex polygons, such as rectangles, circles, etc. It can be represented by transforming ε. When $\varepsilon = 1$, $a_x = b_y$, this expression represents a standard circular equation. If ε is small, you can get a shape that is more like a rectangle.

By generalizing the superellipse, a manipulator expression for grasping contours is obtained in the plane.

$$\begin{cases} x = c \\ y = a_y \cos^{\varepsilon}\omega\cos\theta - a_z \sin^{\varepsilon}\omega\sin\theta + y_1 \\ z = a_y \cos^{\varepsilon}\omega\sin\theta + a_z \sin^{\varepsilon}\omega\cos\theta + z_1 \end{cases} \tag{9}$$

Eq. (9) is defined as a grasping plane expression based on the basic form. Based on the mathematical description of the grasping model, a mathematical expression for the contact plane is reconstructed using the superellipse equation. The position of each finger on the grasping plane is then described qualitatively based on the superellipse equation.

4.2. Grasping algorithm of static analysis and force closure

The actual situation of the robot point contact with the target object is considered. r_i is set as the position vector of the contact point between the i-th finger of the manipulator and the target object relative to the target object coordinate system. For each contact point p_i, the force spiral received can be expressed as Eq. (10).

$$\omega_i = G_i f_i \tag{10}$$

In which, $G_i \in \mathbb{R}^{6\times q_i}$, G is defined as a grasping matrix, which is defined in the Eq. (11) in the case of hard finger contact with friction:

$$G_i = \begin{bmatrix} n_i & o_i & t_i \\ r_i \times n_i & r_i \times o_i & r_i \times t_i \end{bmatrix} \tag{11}$$

In which, n_i is the normal vector within the unit at the contact point p_i, r_i is the position vector of contact p_i in the object coordinate system, o_i and t_i are unit tangent vectors, G_i is the grasping matrix of contact point p_i, ω_i is the contact force spiral at the first contact point p_i.

For the five-finger manipulator, there are five contact points with the target object during grasping operation, so there are five contact force spiral elements that is $m = 5$.

The resultant helix amount $\omega \in \mathbb{R}^6$ applied by the finger can be shown in Eq. (12).

$$\omega = \sum_{i=1}^{m} \omega_i = \sum_{i=1}^{m} G_i f_i = Gf \tag{12}$$

In which, G is the total grasping matrix:

$$G = [G_1 \quad G_2 \quad \cdots \quad G_m] \in \mathbb{R}^{6\times q} \tag{13}$$

In order to stabilize grasping, the definition of force closed grasping is shown in Eq. (14):

$$\omega = -\omega_e = Gf \tag{14}$$

In which, ω_e is the external force spiral on the target object.

A more simple description of the force closure condition is that the contact forces of all fingers must be within the friction

cone at each point. Now it is required that the grasping posture of the manipulator should balance an external force spiral ω_e. According to the requirements of Eq. (14), there will be many groups of f solutions. Therefore, it is necessary to establish relevant evaluation indicators for grasping quality. Further best grasping poses were selected.

4.3. Grasp quality assessment based on grip force spiral space

From different aspects, scholars have proposed indicators for the evaluation of grasping quality, including the characteristics of the object (shape, size, weight), frictional constraints and force closure. These grasping quality evaluations are divided into three categories [40]: 1) calculated from the algebraic properties of grasping matrix G. 2) Calculated from the geometric relations between grasping contact points. 3) Calculate from the spiral space of the grasping force.

The first two types of grasp quality measurement relate to the geometric position of the contact point, but do not take into account any limitations on the force applied to the fingers. Even if the force closure grasper obtained can resist external disturbance forces spiraling in any direction, there is no information on the size of the disturbance that can be resisted. This means that fingers may have to exert a large force to resist a small disturbance in some cases. Therefore, the grasping quality can also be considered when the force exerted by the finger is limited, and the grasping can resist the disturbing force of the screw modulus.

f_i has two common constraints. The first is that the modulus of the force exerted by each finger is individually constrained, which corresponds to each finger having a finite independent power source. For simplicity and without loss of generality, it is assumed that all exponential forces have the same limit and are normalized to 1, i. e., $\| f_i \| \leqslant 1,\ i = 1, 2, ..., n$.

The cone of friction at the contact point is approximated as a prism with m sides, and the applied force represents a prismatic force $f_{ij} (j = 1, 2, ..., m)$ along the positive linear combination of the prism, usually referred to as the primary force. The force helix ω_i generated by f_i at p_i can be expressed as a positive linear combination of the force helix ω_{ij} generated by f_{ij}. Now, n fingers on the given object produce a resulting-force spiral, which can be represented as Eq. (15).

$$\omega_O = \sum_{i=1}^{n} \omega_i = \sum_{i=1}^{n} \sum_{j=1}^{m} \alpha_{ij} \omega_{ij} \tag{15}$$

In which, $\alpha_{ij} \geqslant 0$ and $\sum_{j=1}^{m} \alpha_{ij} \leqslant 1$.

By considering the possible variations of α_{ij}, the set of force helices that can be obtained on the object. $\mathscr{P}$ is the Minkowski of the force helix and the convex hull of ω_{ij}:

$$\mathscr{P} = \mathrm{CH}\left(\bigoplus_{\mathrm{i}=1}^{\mathrm{n}} \{\omega_{\mathrm{i}1}, \ldots, \omega_{\mathrm{im}}\} \right) \tag{16}$$

The second common constraint on finger forces is the sum of the forces exerted modulus by n fingers, which is finite and the loading capacity of all fingers is also finite. Suppose that the load capacity is 1, then the constraint is $\sum_{i=1}^{n} \| f_i \| \leqslant 1$.

By again approximating the friction cone as a pyramid, the grasp force spiral on the object is given by the Eq. (17).

$$\omega = \sum_{i=1}^{n} \sum_{j=1}^{m} \alpha_{ij} \omega_{ij} \tag{17}$$

In which, $\alpha_{ij} \geqslant 0$ and $\sum_{i=1}^{n} \sum_{j=1}^{m} \alpha_{ij} \leqslant 1$.

The set $\mathscr{P}$ is a convex hull of the primordial force spiral ω_{ij}:

$$\mathscr{P} = \mathrm{CH}\left(\bigcup_{\mathrm{i}=1}^{\mathrm{n}} \{\omega_{\mathrm{i}1}, \ldots, \omega_{\mathrm{im}}\} \right) \tag{18}$$

The ensemble $\mathscr{P}$ is called the grasp wrench space (GWS).

Considering the force constraints, the grasping mass metric is defined as the maximum disturbing force spiral that can be resisted in any direction. The distance from the origin of the force helix space to the closed surface of $\mathscr{P}$. Geometrically, the mass evaluation of grasping is equal to the radius of the largest sphere completely contained in $\mathscr{P}$ centered on the origin of the force helix space, so it is often referred to as the criterion of the largest sphere. Grabbing quality is measured by:

$$Q_1 = \min_{\omega \in \partial \mathscr{P}} \| \omega \| \tag{19}$$

In which, $\partial \mathscr{P}$ is the boundary of $\mathscr{P}$.

Q_1 has a clear and useful physical significance for general purpose grasping. However, it depends on the reference system used to calculate the torque. The center of mass of an object is chosen as the origin of the reference system, which is consistent with the dynamics of the system. For other measurements it may be difficult in some cases to know the center of mass exactly.

In order to avoid Q_1 dependence on the reference system for calculating the torque, the radius of the largest sphere of the reference system that can be chosen is used as a measure of mass, but the high complexity of the calculation makes it difficult to realize a large range of applications. To solve this problem, the volume of $\mathscr{P}$ is proposed as the measurement standard of grab mass.

$$Q_2 = \mathrm{Volume}(\mathscr{P}) \tag{20}$$

In which, Q_2 is independent of the reference frame used to calculate torque. Therefore, this paper uses Q_2 as the grasping oriented measurement standard of manipulator.

5. Simulation experiment analysis

In the simulation of the humanoid five-fingered manipulator grasping process, SOLIDWORKS was used to build the manipulator model. Several grasping positions of the manipulator were calculated using external programming algorithms, and then the results and the manipulator model were imported into the ROS environment. Pose screening is performed by means of visualization, inverse motion calculation and collision detection with the simulation software Move It!. The visualization and feasibility verification of the robotic grasping solution is realized.

The humanoid five-finger manipulator has three joints in each finger. In addition to the thumb, the structure of the other four fingers is the same. The joints of each finger can move independently and the whole finger has 15 degrees of freedom. For convenience in Move It!. In this paper, the structure of the manipulator is simplified.

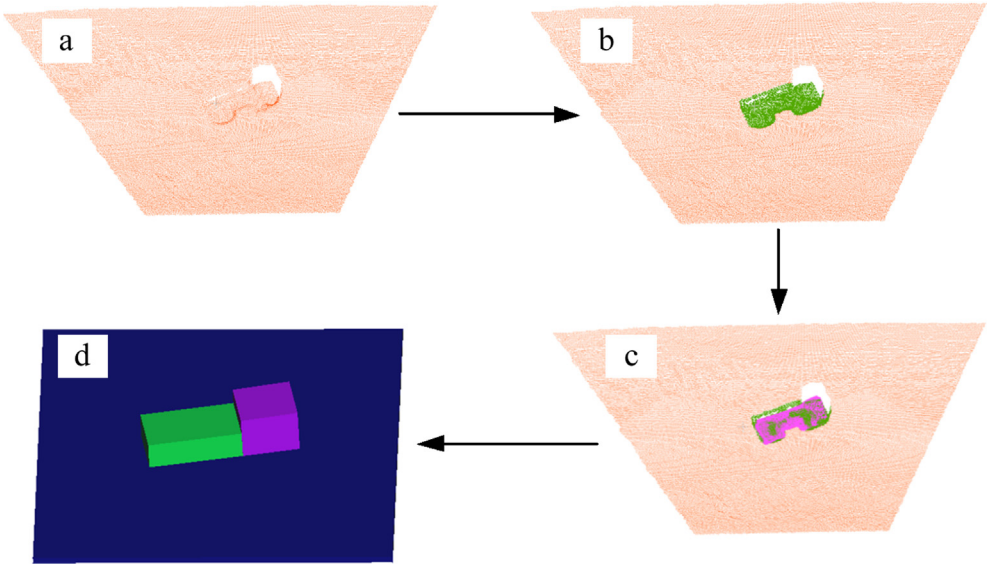

Fig. 8 Pre-processing flow and results of scene simulation analysis.

In order to simplify the capture environment, the scene point cloud was pre-processed, object pose estimated and the scene simplified to obtain the results shown in Fig. 9.

Fig. 8(a) is the cloud map of scenic spots after point cloud pretreatment. Fig. 8(b) shows the point cloud image of the scene after pre-processing, the green point cloud in the figure is the target point cloud. Fig. 8(c) is the result of pose estimation, and purple is the point cloud image obtained by transformation matrix after registration. Then, standard processing of the background point cloud is then performed to facilitate post-processing. Fig. 8(d) shows the simplified scene diagram. A simplified model of the object is mapped to the location of the target object. In the Fig. 8, the blue is flat platform. The green and purple are simplified models of the target object, and they each represent a different part of the target object. Pose positions from different perspectives are selected and placed on the workbench. Virtual work platforms are successively established according to the above processing process, as shown in Fig. 9.

According to the above scheme, the characteristics of the target object are analyzed. Based on the simplified results, the autonomous grasping method of the fundamental body analysis is employed to constrain the grasping position and attitude. The evaluation of the grasping quality in force spiral space is established according to the force closure gripping principle. Finally, the grasping posture of the five-fingered manipulator was obtained, as shown in Fig. 10.

The specific implementation steps are as follows:

1) The priority grasping strategy is set according to the size of the volume. Generally, the part with the largest volume is selected as the first grasping part. Therefore, the grasping planning is first made for the part with the largest volume. When the part is determined to be unable to grasp according to the grasping rules, the grasping analysis is carried out for the part with smaller volume.

2) According to the characteristic plane of the object and the superellipse equation, the grasping plane of the object is determined.

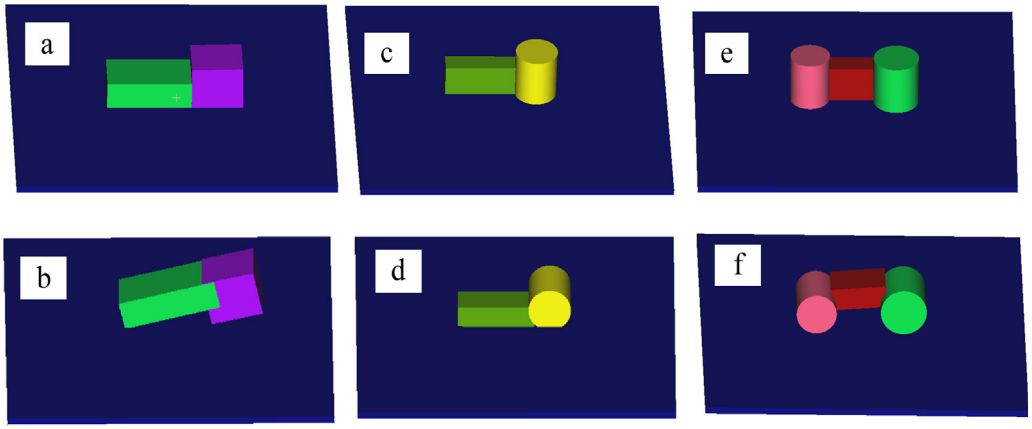

Fig. 9 Simplified virtual simulation workbench (a: views 1 of object 1, b: views 2 of object 1, c: views 1 of object 2, d: views 2 of object 2, e: views 1 of object 3, f: views 2 of object 3).

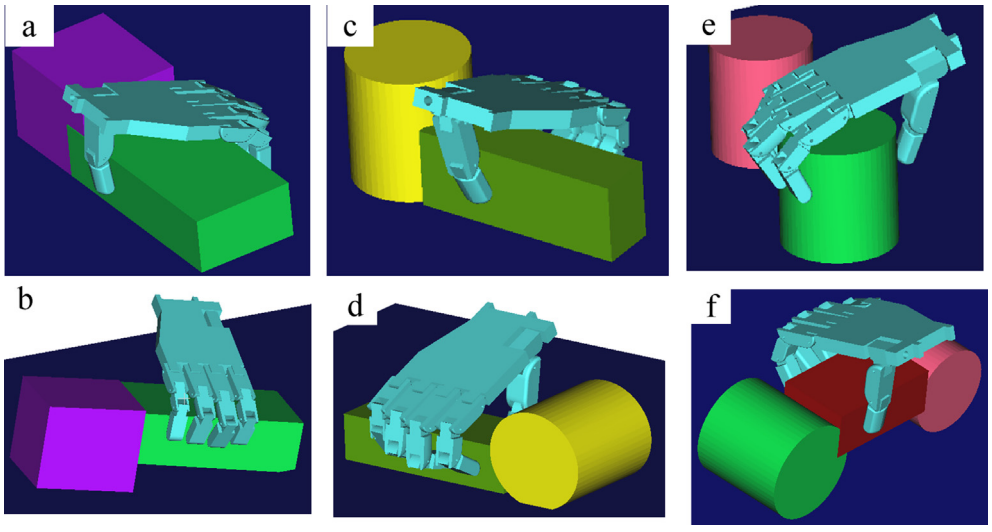

Fig. 10 Simulation results of manipulator grasping posture (a: views 1 of object 1, b: views 2 of object 1, c: views 1 of object 2, d: views 2 of object 2, e: views 1 of object 3, f: views 2 of object 3).

3) According to the grasping principle of the force-closed finger contact force model, the grasping planning of the target is completed and the position of the contact point is determined.

4) Based on the determined position and pose, the parameters of the joints of the manipulator are solved using the Move It! inverse motion solver. Finally, the grasping posture of the manipulator is obtained.

5) With collision detection, interpenetration between virtual objects is avoided and interfering grasping poses are excluded. In actual grasping, constraints formed by object platforms or other objects have an influence on the grasping judgment because the target object pose exists randomly.

6) The optimal grasping posture is selected according to the evaluation criteria for grasp stability. During the validation of the software framework in MoveIt!, grasping planning the task of the target object is completed and the precise grasping pose planning of the target object is realized. The above simulation results prove that the proposed algorithm is reasonable and can be used stably in the virtual environment.

6. Conclusion

This paper proposes a method for determining the grasping posture of a manipulator based on shape analysis and force closure. Using the concave and convex properties of the object, the CPC method is used to segment the target object, which is divided into blocks, and these blocks are fitting to sphere, cylinder, and rectangular shapes. Then the optimal grasping plane of the manipulator is analyzed. An autonomous grasping method based on fundamental form analysis is presented in this paper. Accord to qualitative description of the grasping plane based on a superellipse, the mechanical model of the grasping contact points is analyzed using the characteristic plane of the object fundamental form. The grasping posture is constrained based on the simplified results and the grasping analysis is carried out using force closure to obtain a range of grasping postures for the manipulator. Meanwhile, the optimal grasping attitude is obtained by considering the load range of the manipulator and establishing a grasping quality evaluation mechanism based on the force spiral. This method eliminates the complicated training process and reduces the complexity of the manipulator grasping. Finally, a simulation platform is used to obtain the best grasping posture. Simulation and visualization of the grasping posture of the manipulator is realized.

Data availability statement

The data used to support the findings of this study have not been made available because the relevant data involves legal issues and related confidentiality.

Declaration of Competing Interest

The authors declare that they have no known competing financial interests or personal relationships that could have appeared to influence the work reported in this paper.

Acknowledgments

This work was supported by grants of National Natural Science Foundation of China (Grant Nos. 52075530, 51575407, 51505349, 61733011, 41906177); the Grants of Hubei Provincial Department of Education (D20191105); the Grants of National Defense Pre-Research Foundation of Wuhan University of Science and Technology (GF201705); Open Fund of the Key Laboratory for Metallurgical Equipment and Control of Ministry of Education in Wuhan University of Science and Technology (2018B07, 2019B13) and Open Fund of Hubei Key Laboratory of Hydroelectric Machinery Design & Maintenance in Three Gorges University (2020KJX02).

References

[1] D. Jiang, G. Li, C. Tan, L. Huang, Y. Sun, J. Kong, Semantic segmentation for multiscale target based on object recognition

using the improved Faster-RCNN model, Future Generation Computer Systems 123 (2021) 94–104.
[2] D. Lyu, Z. Chen, Z. Cai, S. Piao, Robot path planning by leveraging the graph-encoded floyd algorithm, Future Generation Computer Systems (122) 122 (2021) 204–208.
[3] Z. Deng, B. Fang, B. He, J. Zhang, An adaptive planning framework for dexterous robotic grasping with grasp type detection, Robotics and Autonomous Systems (3) 140 (2021) 103727, https://doi.org/10.1016/j.robot.2021.103727.
[4] J. Hu, Y. Sun, G. Li, G. Jiang, B. Tao, Probability analysis for grasp planning facing the field of medical robotics, Measurement 141 (2019) 227–234.
[5] H. Chanal, J. Guyon, A. Koessler, Q. Dechambre, B. Boudon, B. Blaysat, N. Bouton, Geometrical defect identification of a SCARA robot from a vector modeling of kinematic joints invariants, Mechanism and Machine Theory 162 (2021) 339.
[6] R. Ma, L. Zhang, G. Li, D. Jiang, S. Xu, D. Chen, Grasping force prediction based on sEMG signals, Alexandria Engineering Journal 59 (3) (2020) 1135–1147.
[7] Y. Sun, C. Xu, G. Li, W. Xu, J. Kong, D. Jiang, B. Tao, D. Chen, Intelligent human computer interaction based on non redundant EMG signal, Alexandria Engineering Journal 59 (3) (2020) 1149–1157.
[8] Y.i. Gan, B. Zhang, C. Ke, X. Zhu, W. He, T. Ihara, Research on robot motion planning based on RRT algorithm with nonholonomic constraints, Neural Processing Letters 53 (4) (2021) 3011–3029.
[9] Y. Sun, Y. Weng, B. Luo, G. Li, B. Tao, D. Jiang, D. Chen, Gesture recognition algorithm based on multi-scale feature fusion in RGB-D images, IET Image Processing 14 (15) (2020) 3662–3668.
[10] L. Massari, M. Calogero, E. Sinibaldi, R. Detry, J. Bowkett, K. Carpenter, Tactile sensing and control of robotic manipulator integrating fiber bragg grating strain-sensor, Frontiers in Neurorobotics 13 (2019) 8.
[11] F. Xiao, G. Li, D. Jiang, Y. Xie, J. Yun, Y. Liu, L. Huang, Z. Fang, An effective and unified method to derive the inverse kinematics formulas of general six-DOF manipulator with simple geometry, Mechanism and Machine Theory 159 (2021) 104265.
[12] A. Tejani, R. Kouskouridas, A. Doumanoglou, D. Tang, T.K. Kim, Latent-class hough forests for 6 DOF object pose estimation, IEEE Transactions on Pattern Analysis and Machine Intelligence 40 (1) (2017) 119–132.
[13] D. Jiang, Z. Zheng, G. Li, Y. Sun, J. Kong, G. Jiang, H. Xiong, B. Tao, S. Xu, H. Yu, H. Liu, Z. Ju, Gesture recognition based on binocular vision, Cluster Computing 22 (S6) (2019) 13261–13271, https://doi.org/10.1007/s10586-018-1844-5.
[14] D. Jiang, G. Li, Y. Sun, J. Kong, B. Tao, D. Chen, Grip strength forecast and rehabilitative guidance based on adaptive neural fuzzy inference system using sEMG, Personal and Ubiquitous Computing (2019), https://doi.org/10.1007/s00779-019-01268-3.
[15] S. Levine, P. Pastor, A. Krizhevsky, J. Ibarz, D. Quillen, Learning hand-eye coordination for robotic grasping with deep learning and large-scale data collection, International Journal of Robotics Research 37 (4-5) (2018) 421–436.
[16] Y. Cheng, G. Li, M. Yu, D. Jiang, J. Yun, Y. Liu, Y. Liu, D. Chen, Gesture recognition based on surface electromyography-feature image, Concurrency and Computation: Practice and Experience 33 (6) (2021) e6051.
[17] D. Jiang, G. Li, Y. Sun, J. Kong, B. Tao, Gesture recognition based on skeletonization algorithm and CNN with ASL database, Multimedia Tools and Applications 78 (21) (2019) 29953–29970.
[18] A. Sahbani, S. El-Khoury, P. Bidaud, An overview of 3d object grasp synthesis algorithms, Robotics and Autonomous Systems 60 (3) (2012) 326–336.
[19] J. Bohg, A. Morales, T. Asfour, Data-driven grasp synthesis-a survey, IEEE Transactions on Robotics 30(2) (2014) 289-309.
[20] K. Hang, M. Li, J. Stork, Hierarchical fingertip space: a unified framework for grasp planning and in-hand grasp adaptation, IEEE Transactions on Robotics 32 (4) (2016) 960–972.
[21] I. Lenz, H. Lee, A. Saxena, Deep learning for detecting robotic grasps, The International Journal of Robotics Research 34 (4-5) (2015) 705–724.
[22] F.-J. Chu, R. Xu, P.A. Vela, Real-world multiobject, multigrasp detection, IEEE Robotics and Automation Letters 3 (4) (2018) 3355–3362.
[23] C. Wenceslao, D. Oetomo, C. Manzie, Tactile-based blind grasping: a discrete-time object manipulation controller for robotic hands, IEEE Robotics and Automation Letters 3 (2) (2018) 1064–1071.
[24] D. Jiang, G. Li, Y. Sun, J. Hu, J. Yun, Y. Liu, Manipulator grabbing position detection with information fusion of color image and depth image using deep learning, Journal of Ambient Intelligence and Humanized Computing (2021), https://doi.org/10.1007/s12652-020-02843-w.
[25] A. Spiers, M. Liarokapis, B. Calli, A. Dollar, Single-grasp object classification and feature extraction with simple robot hands and tactile sensors, IEEE Trans Haptics 9 (2) (2016) 207–220.
[26] B. Luo, Y. Sun, G. Li, D. Chen, Z. Ju, Decomposition algorithm for depth image of human health posture based on brain health, Neural Computing and Applications 32 (10) (2020) 6327–6342.
[27] H. Duan, Y. Sun, W. Cheng, D. Jiang, J. Yun, Y. Liu, Y. Liu, D. Zhou, Gesture recognition based on multi-modal feature weight, Concurrency and Computation: Practice and Experience 33 (5) (2021), https://doi.org/10.1002/cpe.v33.510.1002/cpe.5991.
[28] R. Deimel, O. Brock, A novel type of compliant and underactuated robotic hand for dexterous grasping, International Journal of Robotics Research 35 (1-3) (2016) 161–185.
[29] H. Hemami, Robot hands and the mechanics of manipulation, Automatic Control IEEE Transactions 31 (9) (1986) 879–880.
[30] J. Kerr, B. Roth, Special grasping configurations with dexterous hands[C]// IEEE International Conference on Robotics and Automation, Proceedings. IEEE (1986) 1361-1367.
[31] H. Dai, A. Majumdar, R. Tedrake, Synthesis and optimization of force closure grasps via sequential semidefinite programming [M]//Robotics Research, Springer, Cham, 2018, pp. 285–305.
[32] Y. Mitikiri, K. Mohseni, A geometric framework for rigid body attitude estimation, Automatica 128 (2021) 109494, https://doi.org/10.1016/j.automatica.2021.109494.
[33] G. Li, J. Li, Z. Ju, Y. Sun, J. Kong, A novel feature extraction method for machine learning based on surface electromyography from healthy brain, Neural Computing & Applications 31 (12) (2019) 9013–9022.
[34] S. He, Y. Deng, C. Yan, Z. Gao, C. Lee, A tolerance constrained robot path circular interpolation method for industrial SCARA robots, Proceedings of the Institution of Mechanical Engineers Part B Journal of Engineering Manufacture (4) (2020) 095440542097812.
[35] B. Zuo, W. Qian, A general dynamic force distribution algorithm for multifingered grasping, IEEE Transactions on Systems Man & Cybernetics Part B 30 (1) (2000) 185–192.
[36] Z. Kappassov, J. Corrales, V. Perdereau, Tactile sensing in dexterous robot hands- Review, Robotics and Autonomous Systems (74) 74 (2015) 195–220.
[37] V. Lippiello, B. Siciliano, L. Villani, A grasping force optimization algorithm for multiarm robots with multifingered hands, IEEE Transactions on Robotics 29 (1) (2013) 55–67.
[38] H. Yousef, M. Boukallel, K. Althoefer, Tactile sensing for dexterous in-hand manipulation in robotics-A review, Sensors and Actuators A-Physical 167 (2) (2011) 171–187.
[39] Y. Weng, Y. Sun, D. Jiang, B. Tao, Y. Liu, J. Yun, D. Zhou, Enhancement of real-time grasp detection by cascaded deep

convolutional neural networks, Concurrency and Computation: Practice and Experience 33 (5) (2021) e5976.
[40] A. Máximo, R. Suárez, Grasp quality measures: review and performance, Autonomous robots 38 (1) (2015) 65–88.
[41] S. Liao, G. Li, H. Wu, D. Jiang, Y. Liu, J. Yun, Y. Liu, D. Zhou, Occlusion gesture recognition based on improved SSD, Concurrency and Computation: Practice and Experience 33 (6) (2021) e6063.
[42] C. Tan, Y. Sun, G. Li, G. Jiang, D. Chen, H. Liu, Research on gesture recognition of smart data fusion features in the IoT, Neural Computing and Applications 32 (22) (2020) 16917–16929.
[43] Y. He, G. Li, Y. Liao, Y. Sun, J. Kong, G. Jiang, D. Jiang, B. Tao, S. Xu, H. Liu, Gesture recognition based on an improved local sparse representation classification algorithm, Cluster Computing 22 (S5) (2019) 10935–10946, https://doi.org/10.1007/s10586-017-1237-1.
[44] C. Cardozo, W. Ackooij, L. Capely, Cutting plane approaches for frequency constrained economic dispatch problems, Electric Power Systems Research 156 (MAR) (2018) 54–63.
[45] G. Li, D. Jiang, Y. Zhou, G. Jiang, J. Kong, G. Manogaran, Human lesion detection method based on image information and brain signal, IEEE Access 7 (2019) 11533–11542.
[46] Y. Liu, D. Jiang, H. Duan, Y. Sun, G. Li, B. Tao, J. Yun, Y. Liu, B. Chen, Dynamic gesture recognition algorithm based on 3D convolutional neural network, Computational Intelligence and Neuroscience 2021 (2021) 4828102.